Biodegradability enhancement of a pesticide-containing bio-treated wastewater using a solar photo-Fenton treatment step followed by a biological oxidation process

Vítor J.P. Vilar [a,*], Francisca C. Moreira [a], Ana C.C. Ferreira [a], M.A. Sousa [b,c], C. Gonçalves [b], M.F. Alpendurada [b], Rui A.R. Boaventura [a]

[a] LSRE - Laboratory of Separation and Reaction Engineering - Associate Laboratory LSRE/LCM, Faculdade de Engenharia, Universidade do Porto, Rua Dr. Roberto Frias, 4200-465 Porto, Portugal
[b] IAREN - Water Institute of the Northern Region, Rua Dr. Eduardo Torres 229, 4450-113 Matosinhos, Portugal
[c] Laboratory of Bromatology and Hydrology, Faculty of Pharmacy, University of Porto, Rua Aníbal Cunha 164, 4050-047 Porto, Portugal

ARTICLE INFO

ABSTRACT

This work proposes an efficient combined treatment for the decontamination of a pesticide-containing wastewater resulting from phytopharmaceutical plastic containers washing, presenting a moderate organic load (COD = 1662–1960 $mg\,O_2\,L^{-1}$; DOC = 513–696 $mg\,C\,L^{-1}$), with a high biodegradable organic carbon fraction (81%; BOD_5 = 1350–1600 $mg\,O_2\,L^{-1}$) and a remaining recalcitrant organic carbon mainly due to pesticides. Nineteen pesticides were quantified by LC–MS/MS at concentrations between 0.02 and 45 $mg\,L^{-1}$ (14–19% of DOC). The decontamination strategy involved a sequential three-step treatment: (a) biological oxidation process, leading to almost complete removal of the biodegradable organic carbon fraction; (b) solar photo-Fenton process using CPCs, enhancing the bio-treated wastewater biodegradability, mainly due to pesticides degradation into low-molecular-weight carboxylate anions; (c) and a final polishing step to remove the residual biodegradable organic carbon, using a biological oxidation process. Treatment performance was evaluated in terms of mineralization degree (DOC), pesticides content (LC–MS/MS), inorganic ions and low-molecular-weight carboxylate anions (IC) concentrations. The estimated phototreatment energy necessary to reach a biodegradable wastewater, considering pesticides and low-molecular-weight carboxylate anions concentrations, Zahn-Wellens test and BOD_5/COD ratio, was only 2.3 $kJ_{UV}\,L^{-1}$ (45 min of photo-Fenton at a constant solar UV power of 30 $W\,m^{-2}$), consuming 16 mM of H_2O_2, which pointed to 52% mineralization and an abatement higher than 86% for 18 pesticides. The biological oxidation/solar photo-Fenton/biological oxidation treatment system achieved pesticide removals below the respective detection limits and 79% mineralization, leading to a COD value lower than 150 $mg\,O_2\,L^{-1}$, which is in agreement with Portuguese discharge limits regarding water bodies.

© 2012 Elsevier Ltd. All rights reserved.

---

* Corresponding author. Tel.: +351 918257824; fax: +351 225081674.
  E-mail address: vilar@fe.up.pt (V.J.P. Vilar).

1.   Introduction
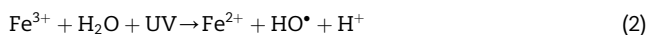
The major sources of pesticide-containing wastewaters include intensive agriculture, associated to pesticide containers and application equipment washing, agricultural industries and pesticide-manufacturing plants (Malato et al., 2000; Ballesteros Martín et al., 2009). The Water Framework Directive (WFD) includes a list of 33 Priority Substances, which represent a significant risk to or via the aquatic environment, including the following water-soluble pesticides: alachlor, atrazine, chlorfenvinphos, chlorpyrifos, diuron, isoproturon, pentachlorophenol and simazine (European Commission, 2008).

Advanced oxidation processes (AOPs) have been recognized as an especially efficient approach to pesticide degradation (Pera-Titus et al., 2004; Gogate and Pandit, 2004a; Devipriya and Yesodharan, 2005). AOPs are chemical oxidation processes characterized by the production of extremely reactive and unselective species such as hydroxyl radicals (HO•), which are able to degrade even the most recalcitrant molecules into biodegradable intermediate compounds or completely mineralize them into CO_2, H_2O and inorganic ions (Gogate and Pandit, 2004a,b). There are many different ways to produce HO•, among which the photo-Fenton process has shown to be the most efficient one for pesticide-containing wastewater treatment (Malato et al., 2002; Oller et al., 2006; Maldonado et al., 2007), achieving higher reaction yields with lower treatment costs, mainly due to a more efficient use of solar light as photon source (Malato et al., 2007). The photo-Fenton system involves the reaction of ferrous ions, Fe^{2+}, and hydrogen peroxide, H_2O_2, to form the active HO• (Fenton process) (Eq. (1)) and, under UV−Vis radiation, Fe^{3+} can be reduced to Fe^{2+} closing a loop mechanism where iron species act as catalyst, giving rise to additional HO• (photo-Fenton process) (Eq. (2)) (Pignatello, 1992). Production of HO• from photocatalytic cleavage of H_2O_2 (Eq. (3)) is not significant, due to the fact that radiation below 280 nm is needed for an effective H_2O_2 cleavage, and borosilicate glass tubes have a cut-off at 280 nm.

$$Fe^{2+} + H_2O_2 \rightarrow Fe^{3+} + HO^- + HO^• \tag{1}$$

$$Fe^{3+} + H_2O + UV \rightarrow Fe^{2+} + HO^• + H^+ \tag{2}$$

$$H_2O_2 + UV \rightarrow HO^• + H^+ \tag{3}$$

In recent years, the coupling between AOPs and biological systems for the treatment of different polluted effluents has been proposed recurrently (Rodriguez et al., 2002; Sarria et al., 2003), including for the treatment of pesticide-containing wastewater (Oller et al., 2007; Farré et al., 2008), where most studies deal with simulated mixtures of a few commercial pesticides (Lapertot et al., 2007; Ballesteros Martín et al., 2009). Success of AOPs/biological oxidation combined treatment relies on reaching an acceptable biodegradability with the shortest photocatalytic oxidation time (optimal treatment time) and subsequently applying a biological oxidation, which turns the overall process cheaper and a more attractive option. Too long oxidation time produces strong degradation

and generates highly oxidized products, with low metabolic value for efficient biological carbon removal, apart from the heavy consumption of H_2O_2. In contrast, a too short oxidation time gives rise to intermediate compounds structurally similar to the parent pesticides, thus still highly toxic and recalcitrant (Malato et al., 2009).

In a previous work, Moreira et al. (submitted for publication) presented an alternative solution for phyto-pharmaceutical plastic containers recycling, consisting of a simple plastic washing with tap water and further treatment of the pesticide-containing wastewater, avoiding the production of hazardous sludge and its disposal in landfills. According to the wastewater characteristics, preliminary elimination of the biodegradable organic carbon fraction was performed in an immobilized biomass reactor (IBR) and different AOPs were tested to achieve pesticide degradation, where the photo-Fenton reaction, with an initial iron dose of 140 mg Fe^{2+} L^{-1}, showed best efficiency.

This study aims to evaluate the possibility of combining a solar photo-Fenton process as pre-oxidation step to enhance the biodegradability of a pesticide-containing wastewater after a preliminary biological treatment, resulting from phytopharmaceutical plastic containers washing, with a further biological oxidation treatment for residual dissolved organic carbon (DOC) removal. Biodegradability assessment is accomplished by the Zahn-Wellens test and BOD_5/COD ratio, and by quantifying low-molecular-weight carboxylate anions and pesticides.

2.   Experimental methodology

2.1.   Chemicals

Photo-Fenton experiments were performed employing iron sulfate heptahydrated (Panreac), hydrogen peroxide (50% (w/v), 1.10 g cm^{-3}, Quimitécnica, S.A.) and sulfuric acid (96%, 1.84 g cm^{-3}, Pronalab) for pH adjustment. The photo-treated wastewater was neutralized with commercial grade sodium hydroxide (30% (w/v), 1.33 g cm^{-3}, Quimitécnica, S.A.). The pH in the biological reactor was controlled by the addition of sodium hydroxide and sulfuric acid. Ultrapure and pure water for the analyses was obtained using a Millipore® system (Direct-Q model) and a reverse osmosis system (Panice®), respectively.

2.2.   Biodegradability assays

Before biological tests and other analyses involving chemical oxidation, the excess hydrogen peroxide present in some samples was removed using a small volume of 0.1 g L^{-1} solution of catalase (2500 U mg^{-1} bovine liver) after adjusting the sample pH to 6.5−7.5. Biochemical oxygen demand (BOD_5) was determined according to OECD-301F test using an OXITOP® system (manometric respirometry) (Clesceri et al., 2005). A 28 days biodegradability Zahn-Wellens test was performed according to the OCDE and EPA guidelines (EMPA, 1992; EPA, 1998). A 250 mL of the pre-treated samples, collected at different photo-Fenton reaction times, without hydrogen peroxide, were added to an open glass vessel, magnetically

stirred and kept in the dark at 25 °C. Activated sludge from Freixo WWTP, Porto, Portugal, previously centrifuged, and mineral nutrients (KH$_2$PO$_4$, K$_2$HPO$_4$, Na$_2$HPO$_4$, NH$_4$Cl, CaCl$_2$, MgSO$_4$ and FeCl$_3$) were added to the samples. The control and blank experiments were prepared using glucose as carbon source, which is highly biodegradable, and distilled water, respectively. Then, the mineral nutrients and the activated sludge were also added. The percentage of biodegradation (D_t) was determined by the following equation (Eq. (4)):

$$D_t = \left[1 - \frac{C_t - C_B}{C_A - C_{BA}}\right] \times 100 \qquad (4)$$

where C_A and C_{BA} are the DOC (mg L^{-1}) in the sample and in the blank, respectively, measured 3 h after starting the experiment, and C_t and C_B are the DOC (mg L^{-1}) in the sample and in the blank, respectively, measured at the sampling time t. The photo-Fenton pre-treated samples are considered biodegradable when D_t is higher than 70% (EMPA, 1992).

2.3. Experimental set-up

2.3.1. Biological oxidation system
The biological oxidation system is composed of a conditioner flat-bottom tank (50 L) and a 45-L immobilized biomass reactor (IBR) (Rocha et al., 2011). The conditioner tank is equipped with a pH control unit (CRISON, electrode and PH27P controller) and a mechanical stirrer (TIMSA) for pH adjustment, using either H$_2$SO$_4$ or NaOH dosed by means of two metering pumps (DOSAPRO MILTON ROY, GTM series, model A). The IBR is a flat-bottom container packed with 62 units of propylene rings (nominal diameter 50 mm), colonized by activated sludge from a municipal wastewater treatment plant (Freixo WWTP). The bioreactor is also equipped with a dissolved oxygen control unit (CRISON, electrode and OXI49P controller) and air is supplied by a blower (compressor-HAILEA model V-20; air flow rate = 20 L min^{-1}; ceramic air diffuser) for maintaining the dissolved oxygen concentration in the system in the selected range (0.5–2 mg O$_2$ L^{-1}).

2.3.2. Solar CPC pilot plant
The photo-Fenton experiments were conducted under sunlight in two pilot plants with compound parabolic collectors (CPCs), installed at the roof of the Chemical Engineering Department, Faculty of Engineering, University of Porto (FEUP), Portugal. The plants have a total irradiation area of 4.16 m^2 and 0.91 m^2, two recirculation tanks (100/50 L and 10/20 L), two recirculation pumps (20 L min^{-1}), two flowmeters, five polypropylene valves, connecting polypropylene tubing and an electric board for process control (Pereira et al., 2011; Rocha et al., 2011). The solar collectors are made-up of 20 and 4 (respectivey for each plant) borosilicate tubes (Schott-Duran type 3.3, Germany, cut-off at 280 nm, internal diameter 46.4 mm, length 1500 mm and thickness 1.8 mm) connected by polypropylene junctions. The pilot plants are operated in batch mode and can be worked in two ways: using the total CPCs area (4.16/0.91 m^2) or using 2.08/0.455 m^2 of CPCs area individually, giving the possibility of performing two different experiments at the same time and at the same solar radiation conditions. The plants are mounted on a south oriented fixed platform tilted 41° (local latitude). The intensity of solar UV

radiation was measured by a global UV radiometer (ACADUS 85-PLS) mounted on the pilot plant at the same angle, which provides data in terms of instantaneous radiation (W$_{UV}$ m^{-2}). Eq. (5) allows to obtain the amount of accumulated UV energy ($Q_{UV,n}$ kJ L^{-1}) received on any surface in the same position with regard to the sun in a time interval Δt per unit of volume of water inside the reactor.

$$Q_{UV,n} = Q_{UV,n-1} + \Delta t_n \overline{UV}_{G,n} \frac{A_r}{V_t}; \quad \Delta t_n = t_n - t_{n-1} \qquad (5)$$

where t_n is the time corresponding to n-water sample, V_t is the total effluent volume, A_r is the illuminated collector surface area and $\overline{UV}_{G,n}$.the average solar ultraviolet radiation measured during the period Δt_n.

2.4. Experimental procedure

2.4.1. Phytopharmaceutical plastic containers wastewater
Phytopharmaceutical plastic containers from VALORFITO, after being granulated into small pieces in EGEO-SISAV-CIRVER facilities, were washed with tap water in a proportion of 0.15 kg of plastics per liter of water. Three washing batches were performed using fresh contaminated plastics in order to obtain enough volume of pesticide-containing wastewater to proceed with the experiments. The main physical/chemical characteristics and the pesticide content of the washing batches wastewater are summarized in Tables 1 and 2, respectively.

2.4.2. First biological oxidation
The biological reactor was inoculated with 80 L of wastewater collected at an aerated activated sludge reactor from Freixo WWTP. After 5 days of recirculation in batch mode at 250 L h^{-1}, biomass was completely fixed on supports, as confirmed by volatile suspended solids (VSS) analysis. The remaining wastewater at the biological reactor (conditioner tank + IBR) was discharged and a volume of 75–86 L of pesticide-containing wastewater was added to the conditioner tank and then pumped to the IBR, which operates as an up-flow reactor at a recirculation rate of 250 L h^{-1} (EHEIM pump) between conditioner tank and IBR. pH was controlled in a range of 6.5–7.5. Three biological pre-treatment batches were performed and resulting wastewaters were mixed. Tables 1 and 2 summarize, respectively, the main physical/chemical characteristics and pesticide content of the mixture.

2.4.3. Solar photo-Fenton process
Two solar photo-Fenton experiments were performed, both using an initial iron dose of 140 mg Fe^{2+} L^{-1} (the optimum iron dose for this wastewater according to the results reported by Moreira et al. (submitted for publication)), one directed to the kinetic study and the other to biodegradability tests. For the photo-Fenton kinetic study experiment, a volume of 16 L of wastewater resulting from biological treatment was added to the recirculation tank of the CPC units (0.455 m^2) and homogenized by turbulent recirculation during 15 min in darkness (a first control sample was taken to characterize the wastewater). The pH was adjusted with sulfuric acid to 2.6–2.9 and another sample was taken after 15 min to confirm the pH. Afterward, iron salt (140 mg Fe^{2+} L^{-1}) was added and well homogenized for 15 min and a third sample was taken for iron

Table 1 – Physical/chemical characteristics of the wastewater resulting from the phytopharmaceutical plastic containers washing immediately after the washing, after the first biological treatment and at the optimal solar photo-Fenton treatment time.

Parameter	Washing	BT1	OSPFT	ELV (Decree-Law no. 236/98)
pH	6.7−7.2	7.6	2.7	6.0−9.0
Conductivity (μS cm^{-1})	739−786	926	np	−
Dissolved oxygen (mg L^{-1})	3.0−3.8	7.2	np	−
Turbidity (NTU)	43−188	92	np	−
COD (mg O$_2$ L^{-1})	1662−1960	892	280	150
DOC (mg C L^{-1})	513−696	303	119	−
BOD$_5$ (mg O$_2$ L^{-1})	1350−1600	160	100	40
BOD$_5$/COD	0.79−0.83	0.18	0.36	−
Total carbon (mg C L^{-1})	536−735	378	127	−
Inorganic carbon (mg C L^{-1})	23−39	75	8.2	−
Polyphenols (mg caffeic acid L^{-1})	16−24	13	np	−
Nitrite (mg NO$_2^-$ L^{-1}/mg N-NO$_2^-$ L^{-1})	5.3/1.6−34/10	7.9/2.4	2.8/0.9	−
Nitrate (mg NO$_3^-$ L^{-1}/mg N-NO$_3^-$ L^{-1})	<0.01/<0.002−32/7.2	<0.01/<0.002	19/4.4	50/11.3
Ammonium (mg NH$_4^+$ L^{-1}/mg N-NH$_4^+$ L^{-1})	33/26−41/32	106/83	59/46	−
Dissolved organic nitrogen (mg N L^{-1})	75−104	21	25	−
Total dissolved nitrogen (mg N L^{-1})	118−144	106	77	15
Dissolved iron (mg (Fe^{2+} + Fe^{3+}) L^{-1})	2.0−2.5	1.3	42	2.0
Sulfate (mg SO$_4^{2-}$ L^{-1})	68−107	134	708	2000
Phosphate (mg PO$_4^{3-}$ L^{-1})	7.5−23	81	5.1	−
Fluoride (mg F$^-$ L^{-1})	0.8−1.9	1.7	2.2	−
Chloride (mg Cl$^-$ L^{-1})	58−92	97	90	−
Bromide (mg Br$^-$ L^{-1})	1.2−5.4	2.9	1.8	−
Lithium (mg Li$^+$ L^{-1})	0.1−0.3	0.3	0.03	−
Sodium (mg Na$^+$ L^{-1})	80−84	87	103	−
Potassium (mg K$^+$ L^{-1})	34−37	66	39	−
Magnesium (mg Mg^{2+} L^{-1})	18−39	40	18	−
Calcium (mg Ca^{2+} L^{-1})	112−128	110	72	−
TSS (mg L^{-1})	62−82	126	np	60
VSS (mg L^{-1})	52−52	104	np	−

Washing: effluent produced; BT1: effluent after the first Biological Treatment; OSPFT: effluent at the Optimal Solar Photo-Fenton Time; np-analysis not performed; ELV: Emission Limit Values.

concentration control. Finally, the first dose of hydrogen peroxide was added, the CPCs were uncovered, and samples were taken at different intervals of time to evaluate the degradation process. The concentration of hydrogen peroxide was maintained in excess, between 200 and 500 mg L^{-1} during the entire reaction, by adding amounts to compensate the consumed ones, as determined by analyses throughout the experiments. Bacardit et al. (2007) showed that supplying H$_2$O$_2$ in multiple small additions, maintaining the H$_2$O$_2$ concentration between 50 and 550 mg H$_2$O$_2$ L^{-1}, improves the oxidation rates, minimizing the consumption of H$_2$O$_2$ per amount of COD oxidized.

For the biodegradability tests, the photo-Fenton experiment was performed using a volume of 32 L (0.91 m^2 of CPC units) and all the parameters (pH = 2.6−2.9; [Fe^{2+}] = 140 mg Fe^{2+} L^{-1}) were maintained with the exception of hydrogen peroxide dose. In this case, a small amount of hydrogen peroxide was added to the photoreactor, and after hydrogen peroxide total consumption, a sample was taken for bioassays and a new dose of hydrogen peroxide was added. This procedure of "addition-total consumption-sample collection-addition" is very important since it prevents any reaction in dark conditions after sample collection, during the storage and possible interferences in the bioassays. Considering this procedure, the experimental data must be

expressed in terms of hydrogen peroxide consumption and not accumulated UV energy per liter of wastewater.

2.4.4. Combined first biological oxidation/solar photo-Fenton/second biological oxidation

Once there was not enough pre-treated wastewater for this experiment, another phytopharmaceutical plastic containers washing similar to the one pointed in Section 2.4.1 was performed, followed by a first biological treatment as described in Section 2.4.2, but in this case using a wastewater volume of 64 L. The solar photo-Fenton reaction was performed as described in Section 2.4.3, using a bio-treated wastewater volume of 62 L in the pilot plant with 2.08 m^2, until consuming the optimal hydrogen peroxide concentration needed to reach the biodegradable threshold. The second biological oxidation was accomplished in the same way than the first one, but employing a volume of 55 L of bio-photo-treated wastewater. The main physical/chemical characteristics and the pesticide content of the wastewater at the different treatment stages are summarized in Tables 3 and 4.

2.5. Analytical determinations

Evaluation of hydrogen peroxide concentration during the photo-Fenton experiment was performed by the

Table 2 – Pesticide content of the wastewater resulting from the phytopharmaceutical plastic containers washing immediately after the washing, after the first biological treatment and at the optimal solar photo-Fenton treatment time.

Pesticides	Washing ($\mu g\,L^{-1}$)	BT1 ($\mu g\,L^{-1}$)	OSPFT ($\mu g\,L^{-1}$)	LOQ ($\mu g\,L^{-1}$)	LOD ($\mu g\,L^{-1}$)
S-Metolachlor	40,652–45,328	32,888	96	50	15
2,4-D	33,552–43,645	36,785	<LOQ	660	200
MCPA	29,052–38,752	33,596	<LOQ	330	100
Imidacloprid	14,837–17,166	15,676	<LOQ	205	62
Alachlor	8741–12,328	7209	28	80	24
Terbuthylazine	8509–10,218	8093	46	30	9
Isoproturon	7423–15,577	11,864	18	50	15
Bentazone	6500–12,300	9780	<LOQ	45	14
Tebuconazole	5801–6104	4636	<LOQ	50	15
Atrazine	5330–13,960	10,110	6	165	50
Linuron	1995–2305	1580	<LOQ	220	67
Metobromuron	1302–1610	1458	<LOQ	115	35
Dimethoate	1200–1980	1459	64	130	39
Diuron	804–1741	1185	<LOQ	90	27
Metribuzin	738–930	702	14	45	14
Metalaxyl	428–624	484	<LOQ	45	14
Chlorotoluron	319–2525	1189	<LOQ	130	39
Simazine	245–684	387	14	70	21
Terbuthylazine-desethyl	20–30	19	324	20	6
Benalaxyl	<LOQ	<LOQ	<LOQ	35	11
Carbaryl	<LOQ	<LOQ	<LOQ	55	17
Carbofuran	<LOQ	<LOQ	<LOQ	25	8
Cymoxanil	<LOQ	<LOQ	<LOQ	250	76
Deisopropylatrazine	<LOQ	<LOQ	<LOQ	225	68
Desethylatrazine	<LOQ	<LOQ	<LOQ	245	74
Methidathion	<LOQ	<LOQ	<LOQ	165	50
Propanil	<LOQ	<LOQ	<LOQ	190	58
Propazine	<LOQ	<LOQ	<LOQ	35	11
Propylene thiourea	<LOQ	<LOQ	<LOQ	1400	424
Pyrimethanil	<LOQ	<LOQ	<LOQ	185	56
Triclopyr	<LOQ	<LOQ	<LOQ	3330	1009

Washing: effluent produced; BT1: effluent after the first Biological Treatment; OSPFT: effluent at the Optimal Solar Photo-Fenton Time; LOQ: Limit of quantification; LOD: Limit of detection; 2,4-D: (2,4-dichlorophenoxy)acetic acid; MCPA: (4-chloro-2-methylphenoxy)acetic acid.

metavanadate method, based on the reaction of hydrogen peroxide with ammonium metavanadate in acidic medium, which results in the formation of a red-orange color peroxovanadium cation, with maximum absorbance at 450 nm (Nogueira et al., 2005). pH and temperature were measured using a pH meter HANNA HI8424. Conductivity was determined by a conductivity meter WTW LF538. Dissolved oxygen was measured by means of a dissolved oxygen meter Crison Oxi 45. Turbidity was measured using a turbidimeter Merck Turbiquant 3000 IR. Chemical Oxygen Demand (COD) was measured by Merck® Spectroquant kits (ref: 1.14541.0001). Dissolved organic carbon (DOC) was measured in a TC-TOC-TN analyzer provided with an NDIR detector and equipped with ASI-V autosampler (Shimadzu, model TOC-V$_{CSN}$), calibrated with standard solutions of potassium hydrogen phthalate (total carbon) and a mixture of sodium hydrogen carbonate/sodium carbonate (inorganic carbon). Dissolved nitrogen was measured in a TC-TOC-TN analyzer coupled with a TNM-1 unit (Shimadzu, model TOC-V$_{CSN}$) calibrated with standard solutions of potassium nitrate and provided by thermal decomposition and NO detection by chemiluminescence method. The total polyphenols concentration was measured by spectrophotometry at 765 nm using the reagent Folin-Ciocalteau (Merck) (Folin and Ciocalteau, 1927).

The polyphenols content is expressed as $mg\,L^{-1}$ of caffeic acid. Iron concentration was determined by colorimetry with 1,10-phenantroline according to ISO 6332. Nitrite, nitrate, sulfate, phosphate, fluoride, chloride, bromide and low-molecular-weight carboxylate anions (acetate, propionate, formate, pyruvate, valerate, malonate, maleate, oxalate, phthalate and citrate) were quantified by ion chromatography (Dionex ICS-2100; column AS 11-HC 4×250 mm; suppressor ASRS®300 4 mm). Ammonium, lithium, sodium, potassium, magnesium and calcium were analyzed by ion chromatography (Dionex DX-120; column: CS12A 4×250 mm; suppressor: CSRS®300 4 mm). Isocratic elution was done with 30 mM NaOH/20 mM methane sulfonic acid, at a flow rate of 1.5/1.0 mL min^{-1}, for anions/cations analyses, respectively. Total suspended solids (TSS) and volatile suspended solids (VSS) were measured by gravimetry, according to the Standard Methods (Clesceri et al., 2005). UV–Vis spectrum between 200 and 700 nm, absorbance at 450 nm (metavanadate method), 510 nm (phenanthroline method) and 254 nm (aromatic content) were obtained using a UNICAM Helios α spectrophotometer. All samples were pre-filtered through 0.45 μm Nylon, VWR membrane filters before analysis. The quantitative analysis of several pesticides was performed by LC–MS/MS. Samples were first diluted (dilution factor of 1/20) and

Table 3 — Physical/chemical characteristics of the pesticide-containing wastewater during the first biological oxidation/solar photo-Fenton/second biological oxidation system assessment.

Parameter	Washing	BT1	SPF	BT2	ELV (Decree-Law no. 236/98)
pH	7.0	7.7	2.7	7.8	6.0—9.0
Conductivity ($\mu S\,cm^{-1}$)	np	np	np	np	—
Dissolved oxygen ($mg\,L^{-1}$)	np	np	np	np	—
Turbidity (NTU)	np	np	np	np	—
COD ($mg\,O_2\,L^{-1}$)	830	622	250	147	150
DOC ($mg\,C\,L^{-1}$)	239	175	75	50	—
BOD_5 ($mg\,O_2\,L^{-1}$)	np	np	np	np	40
BOD_5/COD	np	np	np	np	—
Total carbon ($mg\,C\,L^{-1}$)	274	212	89	79	—
Inorganic carbon ($mg\,C\,L^{-1}$)	36	37	14	29	—
Polyphenols (mg caffeic acid L^{-1})	np	np	np	np	—
Nitrite ($mg\,NO_2^-\,L^{-1}$/$mg\,N\text{-}NO_2^-\,L^{-1}$)	2.7/0.8	2.8/0.8	0.7/0.2	4.0/1.2	—
Nitrate ($mg\,NO_3^-\,L^{-1}$/$mg\,N\text{-}NO_3^-\,L^{-1}$)	<0.01/<0.002	5.8/1.3	0.4/0.1	16/3.6	50/11.3
Ammonium ($mg\,NH_4^+\,L^{-1}$/$mg\,N\text{-}NH_4^+\,L^{-1}$)	27/21	40/31	35/27	25/19	—
Dissolved organic nitrogen ($mg\,N\,L^{-1}$)	60	50	21	30	—
Total dissolved nitrogen ($mg\,N\,L^{-1}$)	81	83	48	54	15
Dissolved iron ($mg\,(Fe^{2+}+Fe^{3+})\,L^{-1}$)	np	np	38	0.5	2.0
Sulfate ($mg\,SO_4^{2-}\,L^{-1}$)	76	92	588	604	2000
Phosphate ($mg\,PO_4^{3-}\,L^{-1}$)	24	30	1.1	20	—
Fluoride ($mg\,F^-\,L^{-1}$)	0.6	1.1	8.2	2.2	—
Chloride ($mg\,Cl^-\,L^{-1}$)	48	54	48	63	—
Bromide ($mg\,Br^-\,L^{-1}$)	<0.05	<0.05	<0.05	<0.05	—
Lithium ($mg\,Li^+\,L^{-1}$)	<0.05	0.2	0.1	<0.05	—
Sodium ($mg\,Na^+\,L^{-1}$)	50	52	47	260	—
Potassium ($mg\,K^+\,L^{-1}$)	30	33	30	46	—
Magnesium ($mg\,Mg^{2+}\,L^{-1}$)	1.1	7.4	2.6	3.8	—
Calcium ($mg\,Ca^{2+}\,L^{-1}$)	73	75	49	54	—
TSS ($mg\,L^{-1}$)	np	np	np	np	60
VSS ($mg\,L^{-1}$)	np	np	np	np	—

Washing: effluent produced; BT1: effluent after the first Biological Treatment; SPF: effluent after the Solar Photo-Fenton treatment; BT2: effluent after the second Biological Treatment; np-analysis not performed; ELV: Emission Limit Values.

subsequently injected in HPLC (Waters Alliance HT 2795; analytical column Waters Atlantis dC18, 3 μm, 2.1 × 100 mm), coupled to a mass spectrometer (Micromass Quattro micro). The mass detector was operated in MRM mode (Multiple Reaction Monitoring), selecting specific transitions for each pesticide, according to the conditions described by Carvalho et al. (2008). The final optimized method allowed the concurrent detection of 31 pesticides, during chromatographic runs 20 min long.

3. Results and discussion

3.1. Wastewater characterization

Tables 1 and 2 show the main physical/chemical characteristics and the pesticide content, respectively, of the wastewater resulting from phytopharmaceutical plastic containers washing, before and after preliminary biological treatment. The pesticide-containing wastewater presents light yellow color, moderate organic load (COD = 1662—1960 $mg\,O_2\,L^{-1}$; DOC = 513—696 $mg\,C\,L^{-1}$), high biodegradability (BOD_5 = 1350—1600 $mg\,O_2\,L^{-1}$; BOD_5/COD = 0.79—0.83), moderate nitrogen content (5.3—34 $mg\,NO_2^-\,L^{-1}$; <0.01—32 $mg\,NO_3^-\,L^{-1}$; 33—41 $mg\,NH_4^+\,L^{-1}$; 75—104 mg dissolved organic nitrogen L^{-1}; 118—144 mg total dissolved nitrogen L^{-1}), low polyphenols

concentration (16—24 mg caffeic acid L^{-1}) and moderate conductivity, corroborated by the low/moderate concentration of dissolved iron, sulfate, phosphate, fluoride, chloride, bromide, lithium, sodium, potassium, magnesium and calcium. In terms of pesticide composition, 19 pesticides were quantified according to the described analytic method. Four of these pesticides exhibited a concentration above 10,000 $\mu g\,L^{-1}$ and nine of them presented a concentration between 1000 and 10,000 $\mu g\,L^{-1}$ (in relation to the minimum value of the washing range). Alachlor and atrazine have been banned in Europe (Annex I of Directive 91/414/EEC) by the time the experiments were undertaken however it is to admit that plastic containers from such formulations were kept in stock before submitting to the recycling process. The same explanation can be extended to metobromuron and simazine although the quantities in the effluent were residual in agreement with their older banning from marketing. The pesticide-containing wastewater was submitted to a preliminary biological treatment, using an IBR reactor, leading to almost complete elimination of biodegradable organic carbon fraction, 88—90% of BOD_5, resulting in a COD and DOC decrease of 46—54% and 41—56%, respectively, achieving a final wastewater with low biodegradability (BOD_5/COD = 0.18). The recalcitrant character of the bio-treated wastewater is associated to pesticides content, which showed no significant decrease after biological treatment. However, for some pesticides, such as, S-

Table 4 – Pesticide content of the wastewater during the first biological oxidation/solar photo-Fenton/second biological oxidation system assessment.

Pesticides	Washing	BT1	SPF	BT2	LOQ (μg L^{-1})	LOD (μg L^{-1})
S-Metolachlor	16,526	15,308	<LOQ	<LOQ	50	15
2,4-D	10,864	<LOQ	<LOQ	<LOQ	660	200
MCPA	21,320	<LOQ	<LOQ	<LOQ	330	100
Imidacloprid	1996	1916	<LOQ	<LOQ	205	62
Alachlor	3600	3238	<LOQ	<LOQ	80	24
Terbuthylazine	10,398	8592	<LOQ	<LOQ	30	9
Isoproturon	2970	2510	<LOQ	<LOQ	50	15
Bentazone	52,600	43,984	<LOQ	<LOQ	45	14
Tebuconazole	1150	1142	<LOQ	<LOQ	50	15
Atrazine	7952	7716	<LOQ	<LOQ	165	50
Linuron	608	484	<LOQ	<LOQ	220	67
Metobromuron	<LOQ	<LOQ	<LOQ	<LOQ	115	35
Dimethoate	2688	1702	<LOQ	<LOQ	130	39
Diuron	8646	6092	<LOQ	<LOQ	90	27
Metribuzin	<LOQ	<LOQ	<LOQ	<LOQ	45	14
Metalaxyl	<LOQ	<LOQ	<LOQ	<LOQ	45	14
Chlorotoluron	7114	6058	<LOQ	<LOQ	130	39
Simazine	6236	5026	<LOQ	<LOQ	70	21
Terbuthylazine-desethyl	<LOQ	<LOQ	<LOQ	<LOQ	20	6
Benalaxyl	<LOQ	<LOQ	<LOQ	<LOQ	35	11
Carbaryl	<LOQ	<LOQ	<LOQ	<LOQ	55	17
Carbofuran	<LOQ	<LOQ	<LOQ	<LOQ	25	8
Cymoxanil	<LOQ	<LOQ	<LOQ	<LOQ	250	76
Deisopropylatrazine	<LOQ	<LOQ	<LOQ	<LOQ	225	68
Desethylatrazine	<LOQ	<LOQ	<LOQ	<LOQ	245	74
Methidathion	<LOQ	<LOQ	<LOQ	<LOQ	165	50
Propanil	<LOQ	<LOQ	<LOQ	<LOQ	190	58
Propazine	<LOQ	<LOQ	<LOQ	<LOQ	35	11
Propylene thiourea	<LOQ	<LOQ	<LOQ	<LOQ	1400	424
Pyrimethanil	4220	2222	<LOQ	<LOQ	185	56
Triclopyr	<LOQ	<LOQ	<LOQ	<LOQ	3330	1009

Washing: effluent produced; BT1: effluent after the first Biological Treatment; SPF: effluent after the Solar Photo-Fenton treatment; BT2: effluent after the second Biological Treatment; LOQ: Limit of quantification; LOD: Limit of detection; 2,4-D: (2,4-dichlorophenoxy)acetic acid; MCPA: (4-chloro-2-methylphenoxy)acetic acid.

metolachlor, alachlor and terbuthylazineno, it was observed a 30–40% reduction of its concentration in the IBR, possibly associated with the adsorption on the biofilm. Total dissolved organic nitrogen decreased around 71%, which is explained by its oxidation to ammonium nitrogen (this compound increased around 157%). COD, BOD$_5$, total dissolved nitrogen and TSS parameters values of the raw and bio-treated pesticide-containing wastewater exceeds the discharge limits imposed by Portuguese legislation (Decree-Law no. 236/98) (Table 1).

3.2. Solar photo-Fenton process

According to previous results reported by Moreira et al. (submitted for publication), the photo-Fenton reaction, with an initial iron dose of 140 mg Fe^{2+} L^{-1} (Fig. 1), proved to be the most efficient among all studied solar AOPs, including UV, H$_2$O$_2$/UV, TiO$_2$/UV, TiO$_2$/H$_2$O$_2$/UV and Fe^{2+}/H$_2$O$_2$. Similar results were obtained by different other authors (Malato et al., 2002; Oller et al., 2006; Maldonado et al., 2007). Nineteen pesticides have been removed below the respective quantification limit after only 5 kJ$_{UV}$ L^{-1}, consuming 39 mM H$_2$O$_2$.

Although the initial iron dose was 140 mg Fe^{2+} L^{-1}, dissolved iron concentration during the reaction was in the range of 10–20 mg (Fe^{2+} + Fe^{3+}) L^{-1}, due to the precipitation of FePO$_4$, which will be discussed in the following section.

3.3. Evaluation of combined solar photo-Fenton/biological treatment

In order to assess the biocompatibility of the bio-photo-treated wastewater, it was performed a Zahn-Wellens and other biological oxidation tests, all at different stages of the solar photo-Fenton reaction.

Fig. 2a presents the evolution of DOC, COD and two parameters, AOS (average oxidation state) and COS (carbon oxidation state), which can be used to evaluate the oxidation degree and oxidative process efficiency, respectively (Amat et al., 2007; Arques et al., 2007).

$$AOS = 4 - 1.5 \frac{COD}{DOC} \tag{6}$$

$$COS = 4 - 1.5 \frac{COD}{DOC_0} \tag{7}$$
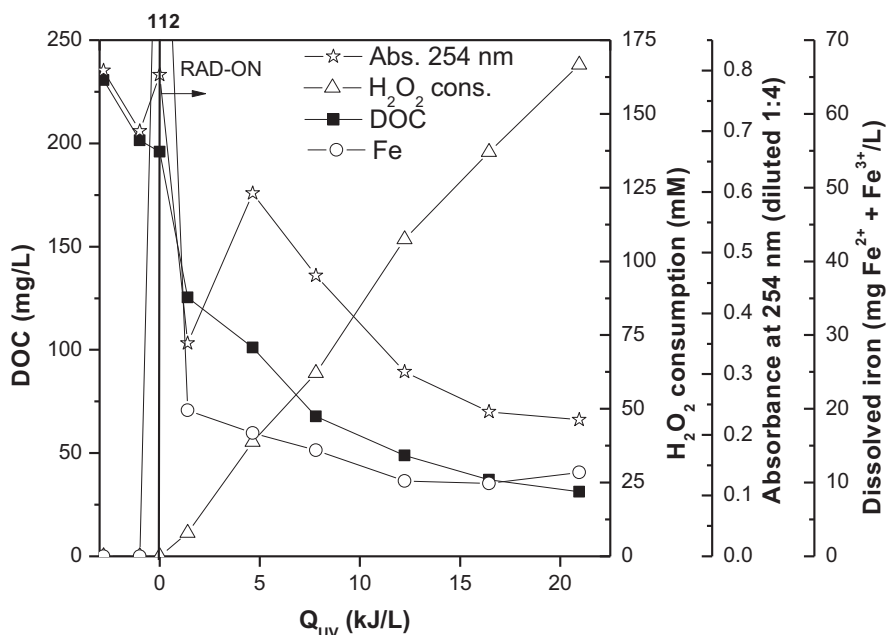
Fig. 1 − Evolution of DOC concentration, H_2O_2 consumption, absorbance at 254 nm and dissolved iron during the solar photo-Fenton process ([Fe^{2+}] = 140 mg L^{-1}; pH = 2.8; kinetic study) as a function of the amount of accumulated UV energy per liter of effluent.

where DOC is the dissolved organic carbon at time t (mg of C L^{-1}), DOC_0 is the initial dissolved organic carbon of the solution (mg of C L^{-1}) and COD is the chemical oxygen demand at time t (mg of O_2 L^{-1}). AOS takes values between +4 for CO_2, the most oxidized state of C, and −4 for CH_4, the most reduced state of C. The AOS only takes into consideration the organic matter in the solution. In COS calculation, CO_2 eliminated from the solution (with an oxidation state +4) is also taken into account.

Thus, they provide indirect information on the biodegradability as they indicate variations in the qualitative composition of the wastewater that could lead to changes in solution biodegradability/toxicity (Scott and Ollis, 1997).

The COD concentration decreased 84%, showing a strong oxidation of the organics, which is well correlated with the COS parameter as it increased from −0.68, indicating the presence of some reduced organic compounds, to +3.3, representing strong mineralization and generation of highly oxidized intermediates. Analyzing the different process phases, more oxidized organic intermediates were formed at the beginning of the process without substantial mineralization, which is corroborated by fast COD decrease and low DOC abatement until H_2O_2 consumption of 5.8 mM. AOS started at −0.68, indicating the presence of more reduced organic compounds, decreased to a minimum of −1.4 after acidification, and increased rapidly until +0.13, suggesting that more oxidized organic intermediates are formed, i.e., until the consumption of 5.8 mM of H_2O_2. After this, AOS reached a plateau of around +0.5 to +0.6. revealing that the chemistry of the intermediates generated during this period does not vary significantly (Sarria et al., 2002). All these variations indicate that there are different intermediates formed, which go through different oxidation−mineralization steps.

Regarding the evaluation of the pesticide concentration during the biodegradability study (Fig. 2b,c), after a H_2O_2 consumption of 38 mM, 18 pesticides were completely removed considering the respective quantification limit of the analytical equipment (exception of terbuthylazine-desethyl, whose concentration increased), representing 0.1% of DOC content (at the beginning of the reaction, pesticides corresponded to 25% of DOC). However, after a consumption of 18 mM of H_2O_2, the 19 pesticides achieved a reduction of at least 96%, attributed to terbuthylazine-desethyl, and 18 of them presented a total removal below the quantification limit, representing 0.3% of DOC. Terbuthylazine-desethyl is a desethylation product of terbuthylazine and, therefore, its concentration increased as terbuthylazine was being degraded (Loos and Niessner, 1999). Terbuthylazine-desethyl concentration rose from an initial value of 104 µg L^{-1}, achieving a maximum value of 2088 µg L^{-1} after a H_2O_2 consumption of 5.8 mM, and then diminished to values below its quantification limit (Fig. 2c).

Low-molecular-weight carboxylate anions concentrations were assessed during the photo-Fenton reaction (Fig. 2d). Pyruvate, valerate and propionate exhibited similar profiles, all presenting low concentration values after the preliminary biological treatment, and showing a fast increase after the beginning of the photo-Fenton reaction, achieving maximum values at 18 mM H_2O_2 consumed (sample 6) (0.8, 3.5 and 75 mg C L^{-1} for pyruvate, valerate and propionate, respectively), and finally decreased to values mostly below the quantification limit. Propionate was the most significant carboxylic acid anion formed during oxidation, corresponding to 63% of DOC after 18 mM H_2O_2 consumption. The maximum pyruvate, valerate and propionate concentration observed coincide with the point where pesticides concentration presents values lower than the quantification limit.
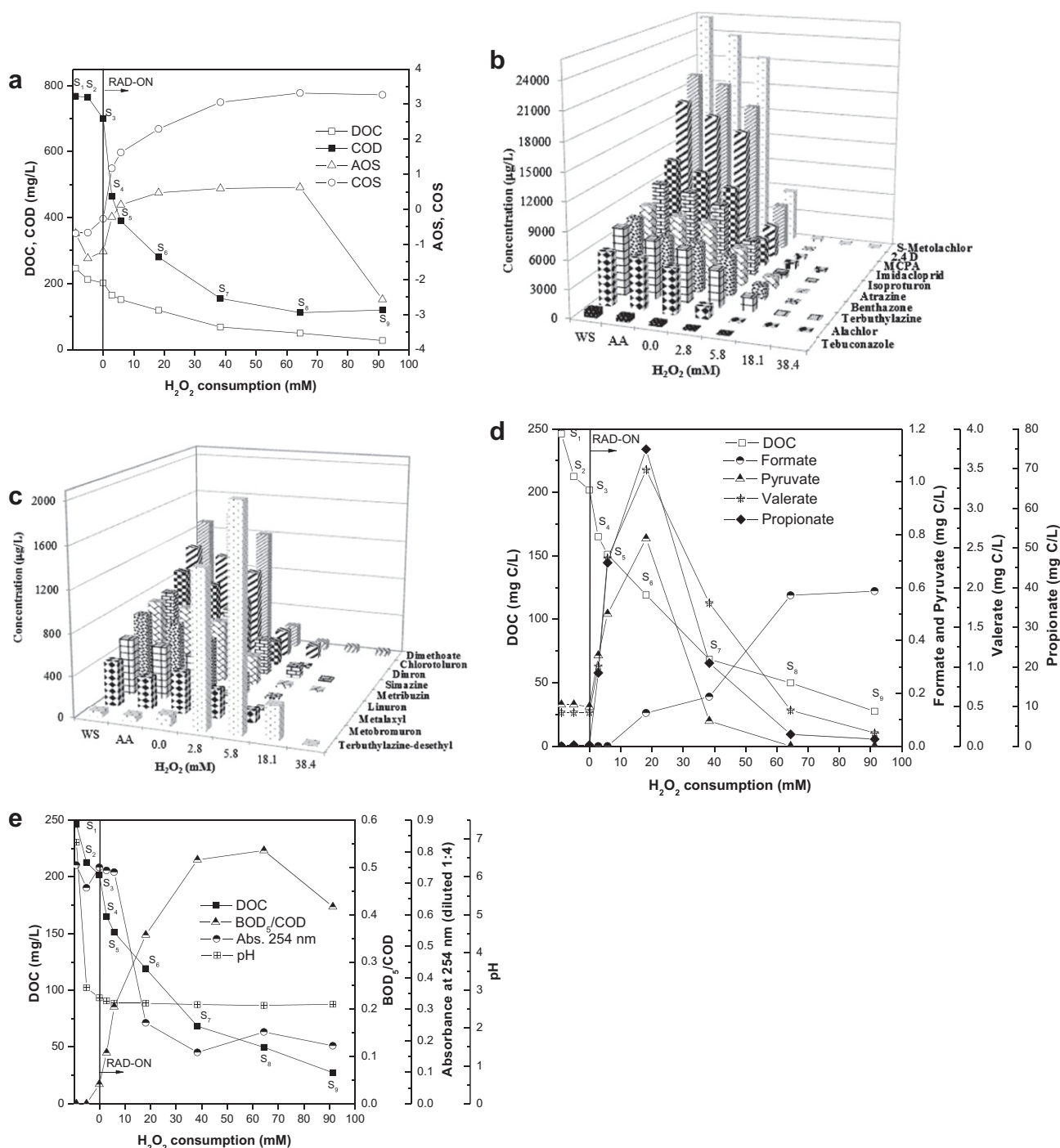
Fig. 2 – DOC, COD, AOS and COS (a); pesticides concentration (b) and (c); low-molecular-weight carboxylate anions concentration (formate, pyruvate, valerate and propionate) (d); BOD$_5$/COD ratio, absorbance at 254 nm and pH (e); evolution as a function of H$_2$O$_2$ consumption during the solar photo-Fenton process ([Fe^{2+}] = 140 mg L^{-1}; pH = 2.8; biodegradability study).

Formate concentration increased continuously during the oxidation reaction, achieving a final concentration of 0.6 mg C L^{-1}, resulting from the oxidation of the other carboxylic acids, since it is the last oxidation product before mineralization to CO$_2$.

BOD$_5$/COD ratio is not affected by the amount or by the oxidation state of organic matter (Amat et al., 2009) and,

therefore, it has been established as a more reliable parameter to evaluate the biodegradability (Marco et al., 1997; Tchobanoglous et al., 2003). Fig. 2e displays a very substantial increase of BOD$_5$/COD, achieving a maximum value after 38 mM H$_2$O$_2$ consumption (BOD$_5$/COD = 0.54), suggesting that photo-oxidation significantly enhanced biodegradability. The aromatic content given by absorbance at 254 nm after dilution
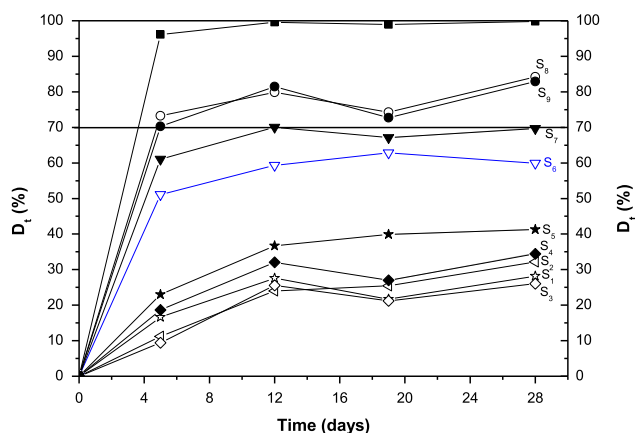
Fig. 3 — Zahn-Wellens test for samples collected during the solar photo-Fenton process (initial sample is also showed, as reference): ☆ - S_1, DOC = 246 mg L^{-1}; ◁ - S_2, DOC = 213 mg L^{-1}; ◇ - S_3, DOC = 202 mg L^{-1}; ◆ - S_4, DOC = 165 mg L^{-1}; ★ - S_5, DOC = 151 mg L^{-1}; ▽ - S_6, DOC = 119 mg L^{-1}; ▼ - S_7, DOC = 68 mg L^{-1}; ○ - S_8, DOC = 50 mg L^{-1}; ● - S_9, DOC = 27 mg L^{-1}; ■ - reference (DOC = 200 mg L^{-1}).

1:4 exhibited a significant decline until a consumption of 18 mM of H_2O_2, related to the degradation of the pesticides (Fig. 2e). pH remained at approximately 2.8 during all experiment (Fig. 2e).

According to the Zahn-Wellens test (Fig. 3), the first five samples (non-treated, after pH adjustment, after iron addition, after 2.8 and 5.8 mM H_2O_2 consumed) revealed a moderate percentage of biodegradation of 28, 32, 26, 34 and 41%, respectively, below the 70% biodegradability threshold defined in Zahn-Wellens test methodology.

However, as expected, the biodegradability of the pesticide-containing bio-treated wastewater was enhanced during the photo-Fenton treatment, reaching 63%, 70%, 82% and 83% after 28 days test, for H_2O_2 doses of 18.1 mM, 38.4 mM, 64.4 mM and 91.3 mM, respectively. Taking into consideration three main factors: (a) pesticide degradation efficiency, which revealed a total removal below the quantification limit for 18 pesticides and a minimum reduction of 96% attributed to terbuthylazine-desethyl, (b) maximum carboxylic acids concentration, which corresponded to the point of pesticides removal below the quantification limit; (c) UV energy and H_2O_2 savings; sample 6 can be considered as corresponding to the optimal phototreatment point to reach a biodegradable effluent. Hence, the optimal energy dose to reach a biodegradable wastewater is 2.3 kJ$_{UV}$ L^{-1}, consuming 18 mM of H_2O_2, as calculated from the kinetic study, and leading to 52% mineralization (DOC$_{final}$ = 119 mg C L^{-1}) and to a total pesticide content removal below the quantification limit for 15 pesticides and a minimum reduction of 94% (excluding the terbuthylazine-desethyl, which concentration has increased), which points to a pesticide content contribution of only 1.6% of DOC.

The characteristics of the wastewater at the optimal solar photo-Fenton time are displayed at Tables 1 and 2 (main physical/chemical characteristics and pesticide content, respectively).

Zapata et al. (2010) reported similar results in the treatment of a real pesticide-contaminated wastewater resulting from the washing of plastic pesticide containers from greenhouses in El Ejido, Almeria (southeastern Spain) for recycling. The containers were shredded and washed, producing rinse water contaminated with pesticides, with an initial DOC ranging between 200 and 500 mg L^{-1}, related to the amount of plastic washed in the same amount of water. In this effluent, it was also possible to detect and quantify twelve pesticides, with the highest individual concentration of about 1000 μg L^{-1}, being necessary 9 and 15 mM of H_2O_2, and no more than 2 and 4 h of illumination, respectively, to achieve almost complete elimination of the pesticides.

The concentration profiles of nitrite, nitrate, ammonium, total dissolved nitrogen and total organic nitrogen during the photo-Fenton reaction are shown in Fig. 4a. All these nitrogen compounds, which set moderate nitrogen content, remained almost constant throughout the treatment. Regarding the total dissolved nitrogen concentration, a first small reduction after acidification can be observed, maybe due to retention of nitrogenated compounds in the foam formed, and a second reduction after H_2O_2 addition, which can be attributed to complexation with iron phosphates. After 5 mM of H_2O_2 consumed, there was a small increase until 18 mM of H_2O_2 consumed, possible related to foam dissolution, and then the concentration remained almost constant between 77 and 80 mg N L^{-1} until the end of the reaction. During all experiment, nitrite, nitrate and ammonium concentrations revealed small increases, ranging from 0.5 to 1.3 mg N-NO$_2^-$ L^{-1}, 3.8—5.1 N-NO$_3^-$ L^{-1} and 44—52 N-NH$_4^+$ L^{-1}, which can be correlated with the degradation of pesticide molecules containing nitrogen atoms, such as alachlor, atrazine, bentazone, chlorotoluron, dimethoate, diuron, imidacloprid, isoproturon, linuron, metalaxyl, among others, which represents a nitrogen content of ca. 12 mg N L^{-1}.

The concentration profiles of chloride, sulfate, phosphate and dissolved iron are exhibited in Fig. 4b. The chloride concentration initially presented values around 74 mg Cl$^-$ L^{-1} and, after the H_2O_2 addition, the concentration started to increase up to ca. 91 mg Cl$^-$ L^{-1}, which can be related to pesticide degradation, containing chlorine atoms, such as, 2,4-(dichlorophenoxy)acetic acid, alachlor, atrazine, S-metolachlor, tebuconazole, among others, which represent a chlorine content of 18 mg Cl$^-$ L^{-1} and close the mass balance. After this point, the chloride concentration remained constant until the end of the reaction.

Sulfate concentration strongly increased from 85 to 385 mg SO$_4^{2-}$ L^{-1} after acidification with sulfuric acid, underwent another high rise to 552 mg SO$_4^{2-}$ L^{-1} after the addition of iron sulfate (140 mg Fe^{2+} L^{-1}) and experienced one last increase to 684 mg SO$_4^{2-}$ L^{-1} after the H_2O_2 addition. According to the amount of acid added (6 mL of H_2SO_4 to 32 L of wastewater) and iron sulfate, the final sulfate concentration should be 650 mg L^{-1}. The pesticides content in term of sulfates, such as, bentazone, dimethoate and metribuzin, is only 4.4 mg L^{-1}, and the other remaining 30 mg L^{-1} can be attributed to the mineralization of other organic compounds containing sulfur atoms. Initially, the pesticide-containing wastewater revealed a phosphate content of about
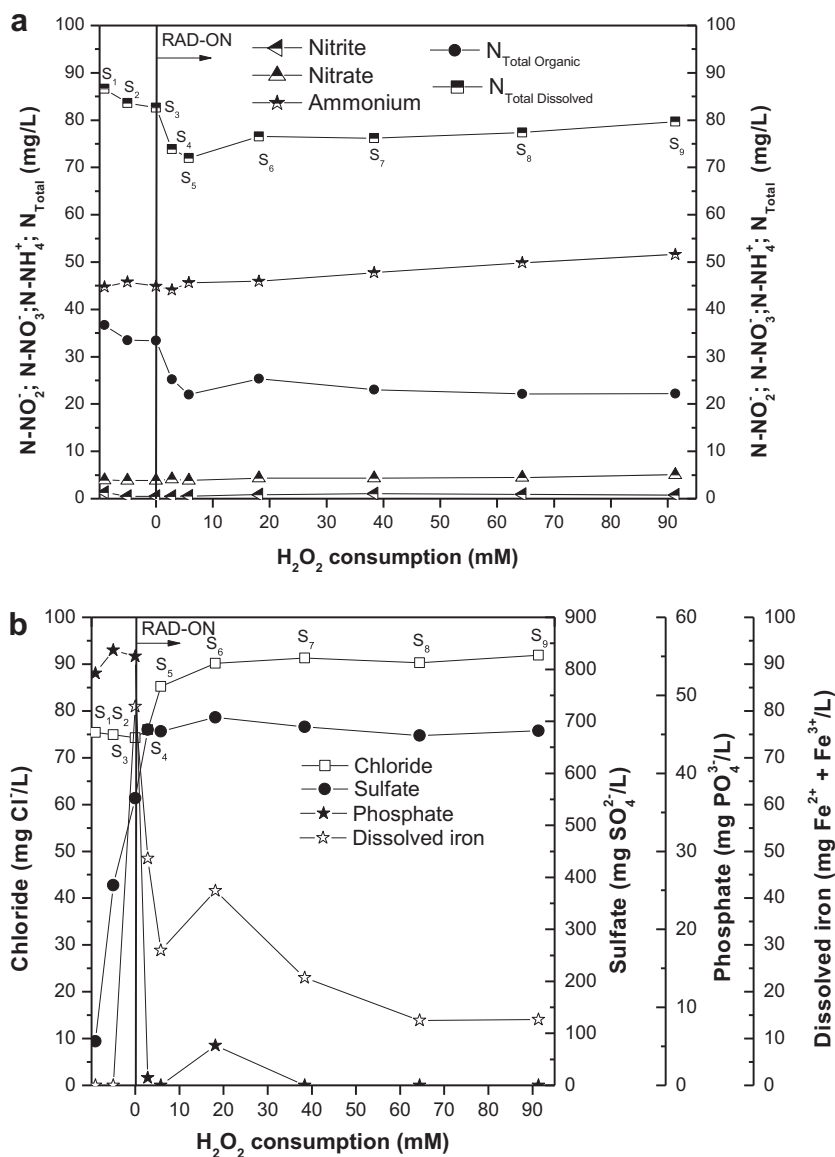
Fig. 4 – Profile of nitrite, nitrate, ammonium, total organic nitrogen and total dissolved nitrogen (a) and chloride, sulfate, phosphate and dissolved iron concentration (b) as a function of the H_2O_2 consumption during the solar photo-Fenton process ($[Fe^{2+}] = 140$ mg L^{-1}; pH = 2.8; biodegradability study).

53–55 mg PO_4^{3-} L^{-1} and after H_2O_2 addition, the phosphate content decreased abruptly to values lower than the detection limit (<0.1 mg L^{-1}). Similarly, the dissolved iron concentration suffered a high reduction after the H_2O_2 addition (64%), which suggests a reaction between the iron ions Fe^{3+} formed according to Eq. (1) and the phosphate ions, PO_4^{3-}, culminating in iron phosphate precipitation (a yellow precipitate in the CPC plant tubes was observed). After 38 mM of H_2O_2 consumed the iron concentration remained almost constant between 14 and 23 mg (Fe^{2+} + Fe^{3+}) L^{-1} during the rest of the experiment.

According to the results reported by Zapata et al. (2009), the presence of both SO_4^{2-} and Cl^- anions did not noticeably reduce the phototreatment time and H_2O_2 consumption in the concentrations range observed in this work.

3.4. Evaluation of solar photo-Fenton/second biological oxidation system

A last experiment was performed combining the three treatment steps: biological oxidation, solar photo-Fenton until the optimum phototreatment time and further biological oxidation. To perform this last experiment, new phytopharmaceutical plastic containers were collected, followed by the same washing procedure. The produced wastewater presents a lower organic load (COD = 830 mg O_2 L^{-1}; DOC = 239 mg C L^{-1}), lower nitrogen content (2.7 mg NO_2^- L^{-1}; <0.01 mg NO_3^- L^{-1}; 27 mg NH_4^+ L^{-1}; 60 mg dissolved organic nitrogen L^{-1}; 81 mg total dissolved nitrogen L^{-1}), lower pesticides content and lower concentration of some ions (mainly magnesium and calcium) (Tables 3 and 4), when compared with the other washing

wastewater. This can be attributed to plastic containers heterogeneity, once they were collected in different occasions. DOC, COD and dissolved organic nitrogen content decreased 27%, 25% and 16%, respectively, in the first biological treatment.

During the complete treatment (first biological oxidation/ solar photo-Fenton/second biological oxidation), DOC and COD values decreased 79 and 82%, respectively, being 53% and 46% due to solar photo-Fenton process, 39% and 36% due to second biological treatment and, 27% and 25% due to first biological treatment, respectively (Fig. 5a). At the end of the treatment, COD value was lower than 150 $mg\,O_2\,L^{-1}$, being in accordance with the discharge limits into receiving water bodies imposed by the Portuguese Legislation (Decree-Law no. 236/98). Fig. 5a also exhibits the low-molecular-weight carboxylate anions concentration during all treatment phases. Formate and pyruvate anions were presented at low concentrations during all phases, $<0.01-0.27\,mg\,C\,L^{-1}$ and $<0.01-0.21\,mg\,C\,L^{-1}$, respectively. Valerate and propionate anions concentration increased during the photo-Fenton oxidation to values around 1.5 and $40\,mg\,C\,L^{-1}$, respectively,

and decreased to values lower than the quantification limit, during the second biological treatment. The low-molecular-weight carboxylic acids anions content represents almost 50% of DOC at the end of the photo-Fenton reaction, being 48% due to propionate.

The photo-Fenton reaction performed until the optimal phototreatment time, considering total pesticide degradation below the quantification limits, consumed 1.8 $kJ_{UV}\,L^{-1}$ of UV radiation and 11 mM of H_2O_2 (lower values than the ones estimated by the biodegradability tests due to the lower pesticide content), achieving 45% mineralization and 46% of DOC was attributed to low-molecular-weight carboxylic anions (Fig. 5a—c). Once again, after H_2O_2 addition, phosphate and dissolved iron content decreased abruptly (Fig. 6), which refers to $FePO_4$ precipitation.

Total dissolved nitrogen content decreased after acidification, due to retention in foam and after H_2O_2 addition, mainly due to complexation with iron phosphates precipitate (Fig. 7). After neutralization of photo-treated wastewater, total nitrogen content increased, due to dissolution of those
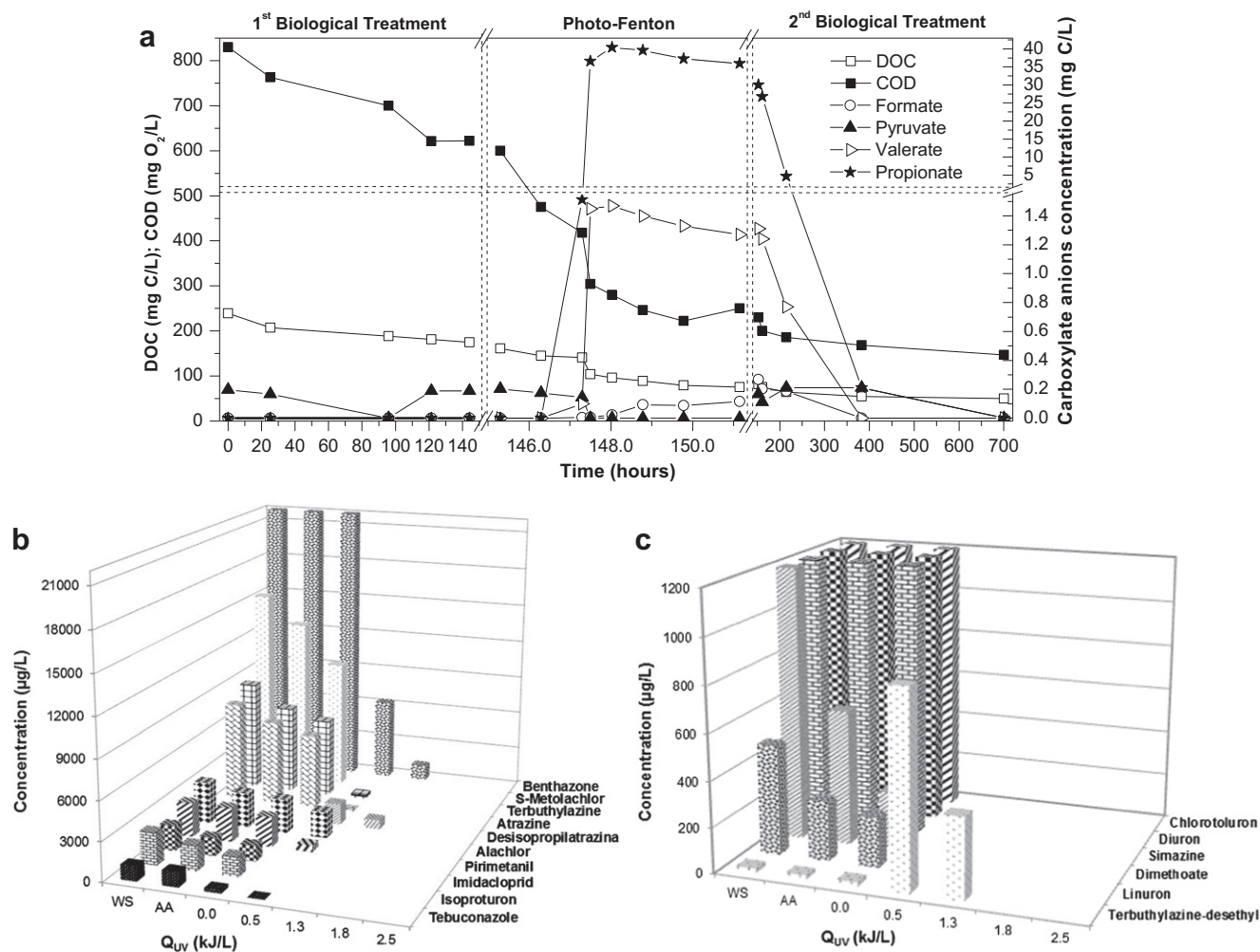

Fig. 5 — (a) DOC, COD, low-molecular-weight carboxylate anions concentration (formate, pyruvate, valerate and propionate) and (b), (c) pesticide content as a function of time during all three treatment steps: first biological oxidation/solar photo-Fenton/second biological oxidation.
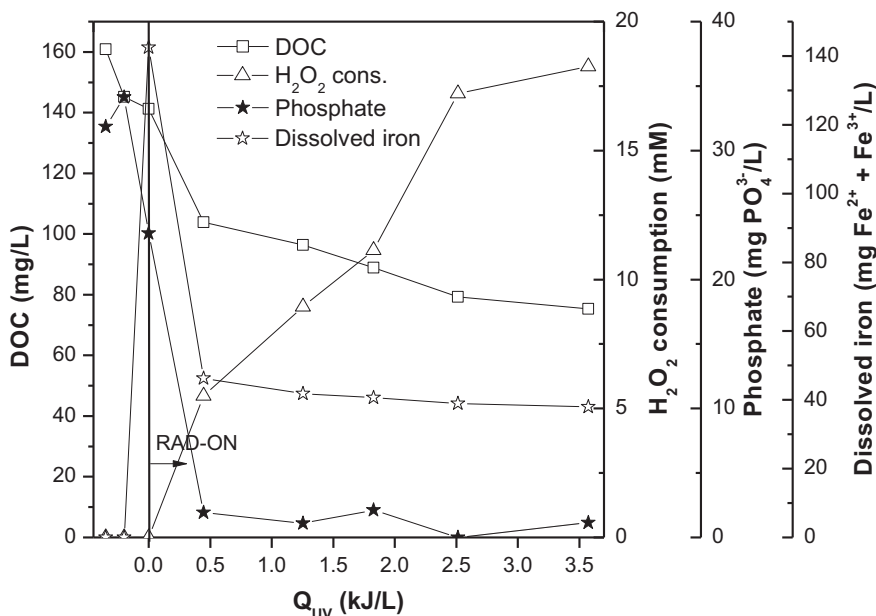
Fig. 6 – DOC, H_2O_2 consumption, phosphate and dissolved iron concentration as a function of the amount of accumulated UV energy per liter of effluent during the solar photo-Fenton reaction.
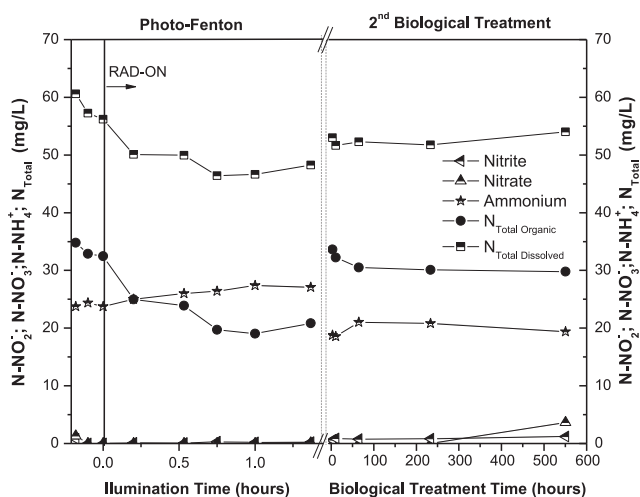

Fig. 7 – Profile of nitrite, nitrate, ammonium, total organic nitrogen and total dissolved nitrogen as a function of time during the solar photo-Fenton and second biological oxidation treatment steps.

enhancing the biodegradability of the wastewater and enabling a subsequent biological oxidation treatment. Mineralization of pesticides was well predicted by inorganic ions concentration, such as chloride, sulfate, ammonium, nitrates and nitrites. The phototreatment energy estimated to reach a biodegradable wastewater was only 2.3 $kJ_{UV} L^{-1}$, consuming 18 mM of H_2O_2, corresponding to 52% mineralization, total pesticide degradation below the quantification limit for 15 pesticides and a reduction of at least 94% (excluding the terbuthylazine-desethyl) and low-molecular-weight carboxylate anions concentration represents 67% of the total DOC. The solar photo-Fenton (62 L; 2.08 m^2 of CPCs)/biological oxidation (55 L) combined system achieved 79% mineralization and total pesticide removal (considering the respective detection limits), achieving a final wastewater with a COD below 150 mg $O_2 L^{-1}$, in agreement with the discharge limits into receiving water bodies imposed by the Portuguese legislation. The initial iron dose necessary for the photo-Fenton reaction depends greatly in the phosphates concentration, which leads to the precipitation of $FePO_4$. This new wastewater, resulting from a new plastic washing presents a lower content in terms of phosphates, which indicates that the initial iron dose used (140 mg $Fe^{2+} L^{-1}$) was higher than the optimum. According to the initial phosphates concentration, a value of 70 mg $Fe^{2+} L^{-1}$ could be enough to achieve the same oxidation efficiency, considering the same accumulated UV energy.

nitrogenated complexes (Fig. 7). Ammonium concentration decreased after neutralization, which can be attribute to the equilibrium NH_4^+/NH_3.

4. Conclusions

The solar photo-Fenton process performed with an initial iron dose of 140 mg $Fe^{2+} L^{-1}$ was found to be very efficient in the treatment of a real pesticide-containing wastewater,

Acknowledgments

REFERENCES

Amat, A.M., Arques, A., Galindo, F., Miranda, M.A., Santos-Juanes, L., Vercher, R.F., Vicente, R., 2007. Acridine yellow as solar photocatalyst for enhancing biodegradability and eliminating ferulic acid as model pollutant. Applied Catalysis B: Environmental 73 (3—4), 220—226.

Amat, A.M., Arques, A., García-Ripoll, A., Santos-Juanes, L., Vicente, R., Oller, I., Maldonado, M.I., Malato, S., 2009. A reliable monitoring of the biocompatibility of an effluent along an oxidative pre-treatment by sequential bioassays and chemical analyses. Water Research 43 (3), 784—792.

Arques, A., Amat, A.M., García-Ripoll, A., Vicente, R., 2007. Detoxification and/or increase of the biodegradability of aqueous solutions of dimethoate by means of solar photocatalysis. Journal of Hazardous Materials 146 (3), 447—452.

Bacardit, J., Oller, I., I.Maldonado, M., Chamarro, E., Malato, S., Esplugas, S., 2007. Simple models for the control of photo-Fenton by monitoring H_2O_2. Journal of Advanced Oxidation Technologies 10 (2), 219—228.

Ballesteros Martín, M.M., Sánchez Pérez, J.A., Casas López, J.L., Oller, I., Malato Rodríguez, S., 2009. Degradation of a four-pesticide mixture by combined photo-Fenton and biological oxidation. Water Research 43 (3), 653—660.

Carvalho, J.J., Jerónimo, P.C.A., Gonçalves, C., Alpendurada, M.F., 2008. Evaluation of a multiresidue method for measuring fourteen chemical groups of pesticides in water by use of LC-MS-MS. Analytical and Bioanalytical Chemistry 392 (5), 955—968.

Clesceri, L.S., Greenberg, A.E., Eaton, A.D., 2005. Standard Methods for Examination of Water & Wastewater, 21st ed. American Public Health Association (APHA), American Water Works Association (AWWA) & Water Environment Federation (WEF).

Decree-Law no. 236/98 de 1 de agosto Pages 3676-3722 in Ministério do Ambiente, Diário da República - I Série-A, No. 176.

Devipriya, S., Yesodharan, S., 2005. Photocatalytic degradation of pesticide contaminants in water. Solar Energy Materials and Solar Cells 86 (3), 309—348.

EMPA, 1992. OCDE Guideline for Testing of Chemicals, Adopted by the Council on 17th July 1992, Zahn-Wellens/EMPA Test. Swiss Federal Laboratories for Materials Testing and Research.

EPA, 1998. U.S. Environmental Protection Agency, Prevention Pesticides and Toxic Substances (7101). Fates, Transport and Transformation Test Guidelines OPPTS 835.3200 Zahn-Wellens/EMPA test. EPA 712-C-96-084. EPA, Washington, DC.

European Commission, 2008. Directive 2008/105/EC of the European Parliament and of the Council of 16 December 2008 on environmental quality standards in the field of water policy, amending and subsequently repealing council directives 82/176/EEC, 83/513/EEC, 84/156/ECEC, 84/491/EEC, 86/280/EEC and amending directive 2000/60/EC of the European Parliament and of the Council.

Farré, M.J., Maldonado, M.I., Gernjak, W., Oller, I., Malato, S., Domènech, X., Peral, J., 2008. Coupled solar photo-fenton and biological treatment for the degradation of diuron and linuron herbicides at pilot scale. Chemosphere 72 (4), 622—629.

Folin, O., Ciocalteau, V., 1927. On tyrosine and tryptophan determinations in proteins. Journal of Biological Chemistry 73, 627—650.

Gogate, P.R., Pandit, A.B., 2004a. A review of imperative technologies for wastewater treatment I: oxidation technologies at ambient conditions. Advances in Environmental Research 8 (3—4), 501—551.

Gogate, P.R., Pandit, A.B., 2004b. A review of imperative technologies for wastewater treatment II: hybrid methods. Advances in Environmental Research 8 (3—4), 553—597.

Lapertot, M., Ebrahimi, S., Dazio, S., Rubinelli, A., Pulgarin, C., 2007. Photo-fenton and biological integrated process for degradation of a mixture of pesticides. Journal of Photochemistry and Photobiology A: Chemistry 186 (1), 34—40.

Loos, R., Niessner, R., 1999. Analysis of atrazine, terbuthylazine and their *n*-dealkylated chloro and hydroxy metabolites by solid-phase extraction and gas chromatography—mass spectrometry and capillary electrophoresis—ultraviolet detection. Journal of Chromatography A 835 (1—2), 217—229.

Malato, S., Blanco, J., Richter, C., Maldonado, M.I., 2000. Optimization of pre-industrial solar photocatalytic mineralization of commercial pesticides: application to pesticide container recycling. Applied Catalysis B: Environmental 25 (1), 31—38.

Malato, S., Blanco, J., Cáceres, J., Fernández-Alba, A.R., Agüera, A., Rodríguez, A., 2002. Photocatalytic treatment of water-soluble pesticides by photo-Fenton and tio2 using solar energy. Catalysis Today 76 (2—4), 209—220.

Malato, S., Blanco, J., Alarcón, D.C., Maldonado, M.I., Fernández-Ibáñez, P., Gernjak, W., 2007. Photocatalytic decontamination and disinfection of water with solar collectors. Catalysis Today 122 (1—2), 137—149.

Malato, S., Fernández-Ibáñez, P., Maldonado, M.I., Blanco, J., Gernjak, W., 2009. Decontamination and disinfection of water by solar photocatalysis: recent overview and trends. Catalysis Today 147 (1), 1—59.

Maldonado, M.I., Passarinho, P.C., Oller, I., Gernjak, W., Fernández, P., Blanco, J., Malato, S., 2007. Photocatalytic degradation of EU priority substances: a comparison between TiO_2 and Fenton plus photo-Fenton in a solar pilot plant. Journal of Photochemistry and Photobiology A: Chemistry 185 (2—3), 354—363.

Marco, A., Esplugas, S., Saum, G., 1997. How and why combine chemical and biological processes for wastewater treatment. Water Science and Technology 35 (4), 321—327.

Moreira, F.C., Vilar, V.J.P., Ferreira, A.C.C., Santos, F.R.A., Dezotti, M., Sousa, M.A., Gonçalves, C., Boaventura, R.A.R., Alpendurada, M.F. Treatment of a wastewater resulting from washing of phytopharmaceutical plastic containers using combined biological and solar-driven advanced oxidation processes at pilot scale. Chemical Engineering Journal, submitted for publication.

Nogueira, R.F.P., Oliveira, M.C., Paterlini, W.C., 2005. Simple and fast spectrophotometric determination of H_2O_2 in photo-Fenton reactions using metavanadate. Talanta 66 (1), 86—91.

Oller, I., Gernjak, W., Maldonado, M.I., Pérez-Estrada, L.A., Sánchez-Pérez, J.A., Malato, S., 2006. Solar photocatalytic degradation of some hazardous water-soluble pesticides at pilot-plant scale. Journal of Hazardous Materials 138 (3), 507—517.

Oller, I., Malato, S., Sánchez-Pérez, J.A., Maldonado, M.I., Gassó, R., 2007. Detoxification of wastewater containing five common pesticides by solar AOPs—biological coupled system. Catalysis Today 129 (1—2), 69—78.

Pera-Titus, M., García-Molina, V., Baños, M.A., Giménez, J., Esplugas, S., 2004. Degradation of chlorophenols by means of advanced oxidation processes: a general review. Applied Catalysis B: Environmental 47 (4), 219–256.

Pereira, J.H.O.S., Vilar, V.J.P., Borges, M.T., González, O., Esplugas, S., Boaventura, R.A.R., 2011. Photocatalytic degradation of oxytetracycline using TiO_2 under natural and simulated solar radiation. Solar Energy 85 (11), 2732–2740.

Pignatello, J.J., 1992. Dark and photoassisted iron(3+)-catalyzed degradation of chlorophenoxy herbicides by hydrogen peroxide. Environmental Science & Technology 26 (5), 944–951.

Rocha, E.M.R., Vilar, V.J.P., Fonseca, A., Saraiva, I., Boaventura, R.A.R., 2011. Landfill leachate treatment by solar-driven AOPs. Solar Energy 85 (1), 46–56.

Rodriguez, M., Sarria, V., Esplugas, S., Pulgarin, C., 2002. Photo-Fenton treatment of a biorecalcitrant wastewater generated in textile activities: biodegradability of the photo-treated solution. Journal of Photochemistry and Photobiology A: Chemistry 151 (1–3), 129–135.

Sarria, V., Parra, S., Adler, N., Peringer, P., Benitez, N., Pulgarin, C., 2002. Recent developments in the coupling of photoassisted and aerobic biological processes for the treatment of biorecalcitrant compounds. Catalysis Today 76 (2–4), 301–315.

Sarria, V., Kenfack, S., Guillod, O., Pulgarin, C., 2003. An innovative coupled solar-biological system at field pilot scale for the treatment of biorecalcitrant pollutants. Journal of Photochemistry and Photobiology A: Chemistry 159 (1), 89–99.

Scott, J.P., Ollis, D.F., 1997. Integration of chemical and biological oxidation processes for water treatment: II. Recent illustrations and experiences. Journal of Advanced Oxidation Technologies 2 (3), 374–381.

Tchobanoglous, G., Burton, F.L., Stensel, D.Metcalf & Eddy, Inc, 2003. Wastewater Engineering: Treatment and Reuse. McGraw-Hill.

Zapata, A., Oller, I., Bizani, E., Sánchez-Pérez, J.A., Maldonado, M.I., Malato, S., 2009. Evaluation of operational parameters involved in solar photo-fenton degradation of a commercial pesticide mixture. Catalysis Today 144 (1–2), 94–99.

Zapata, A., Oller, I., Sirtori, C., Rodríguez, A., Sánchez-Pérez, J.A., López, A., Mezcua, M., Malato, S., 2010. Decontamination of industrial wastewater containing pesticides by combining large-scale homogeneous solar photocatalysis and biological treatment. Chemical Engineering Journal 160 (2), 447–456.